

Discrete Lorentz surfaces and s-embeddings II: maximal surfaces

Niklas Christoph Affolter^{*†}, Felix Dellinger[†],
Christian Müller[†], Denis Polly[†], Nina Smeenk^{*},

December 2, 2024

Abstract

S-embeddings were introduced by Chelkak as a tool to study the conformal invariance of the thermodynamic limit of the Ising model. Moreover, Chelkak, Laslier and Russkikh introduced a lift of s-embeddings to Lorentz space, and showed that in the limit the lift converges to a maximal surface. They posed the question whether there are s-embeddings that lift to maximal surfaces already at the discrete level, before taking the limit. We answer this question in the positive. In a previous paper we identified a subclass of s-embeddings – isothermic s-embeddings – that lift to (discrete) S-isothermic surfaces, which were introduced by Bobenko and Pinkall as a discretization of isothermic surfaces. In this paper we identify a special class of isothermic s-embeddings that correspond to discrete S-maximal surfaces, translating an approach of Bobenko, Hoffmann and Springborn introduced for discrete S-minimal surfaces in Euclidean space. Additionally, each S-maximal surface comes with a 1-parameter family of associated surfaces that are isometric. This enables us to obtain an associated family of s-embeddings for each maximal s-embedding. We show that the Ising weights are constant in the associated family.

^{*}TU Berlin, Institute of Mathematics, Straße des 17. Juni 136, 10623 Berlin, Germany. *E-mail addresses:* `affolter at posteo.net`, `smeenk at math.tu-berlin.de`

[†]TU Wien, Institut of Discrete Mathematics and Geometry, Wiedner Hauptstr. 8-10/104, A-1040 Vienna, Austria. *E-mail addresses:* `felix.dellinger`, `christian.mueller`, `denis.polly at tuwien.ac.at`

Contents

1	Introduction	3
2	Smooth maximal surfaces	5
3	Isothermic congruences	6
4	Isothermic incircular nets	7
5	Koebe congruences	9
6	Christoffel dual	10
7	Maximal surfaces	11
8	Weierstraß representation	12
9	The associated family	14
10	The associated congruences	16
11	The X -variables in the associated family	21

1 Introduction

This paper is the second in a series of two papers, the first being [ADM⁺24]. The goal of the series is to relate recent developments in statistical mechanics to (not quite so recent) developments in discrete differential geometry. A brief introduction to the two topics can be found in [ADM⁺24].

Let us explain which developments we are referring to. An *incircular net* is a map from a quad graph to the plane, such that each quad has an incircle. Chelkak [Che18] used incircular nets to investigate properties of the (planar) *Ising model*, calling them *s-embeddings*. Moreover, he introduced a way to define the coupling constants of an Ising model given an incircular net. He then introduced a way to lift an incircular net to Lorentz space $\mathbf{L}^3 = \mathbb{R}^{2,1}$. Surprisingly, the properties of the Ising model are invariant under isometries of \mathbf{L}^3 . Moreover, he showed (under additional assumptions) that in the thermodynamic limit the lift converges to a maximal surface. Similar constructions and results were obtained by Chelkak, Laslier and Russkikh [CLR23, CLR21] for the dimer model using *conical nets*, also called *t-embeddings* or *Coulomb gauges* [KLRR22] in the statistical mechanics community. However, in this paper we will focus on incircular nets. A question posed in [CLR21] was whether the lifts of some conical nets or incircular nets can be understood as maximal surfaces before taking the limit, as *discrete maximal surfaces*. In this paper we show that the answer is: *yes*.

In the first paper [ADM⁺24], we investigated the geometric properties of the Lorentz lift introduced by Chelkak. The Lorentz lift of a quad of an incircular net is a quad in $\mathbb{R}^{2,1}$ such that each edge is isotropic (also called lightlike). We showed that

- (i) in each quad there is a unique timelike Lorentz sphere that contains all four edges of the quad;
- (ii) at each vertex there is a null-sphere (a sphere of radius zero) that contains the isotropic lines of the four incident edges;
- (iii) at each edge the two incident timelike spheres are touching and the apices of the incident null-spheres lie on both incident timelike spheres.

We call the resulting congruence of spheres a *null congruence*, and we showed that every null congruence is the Lorentz lift of an incircular net. In particular, the incircles of the incircular net are the orthogonal projections of the smallest Euclidean circles (the contours) of the corresponding timelike spheres, the vertices of the incircular net are the projections of the apices of the null-spheres, and the edges of the incircular net are projections of the common isotropic line of the two null-spheres and the two timelike spheres.

Subsequently, we introduced a special class of null congruences which we call *isothermic congruences*. They are characterized by the planarity of the four centers of the timelike spheres around each vertex. The corresponding *isothermic incircular net* has the following property: if for every edge we take the other tangent to the two adjacent incircles, the collection of all these other tangents also constitutes an incircular net. Why do we call these congruences isothermic congruences? There is a well-known discretization of isothermic surfaces called *S-isothermic nets* [BP99, BHS06]. We showed that isothermic congruences are in 2:1 correspondence with S-isothermic nets, hence, there is a special case of incircular nets that does correspond to isothermic surfaces at the discrete level.

In the first part of this paper, we take the specialization sequence one step further. In particular, it is well known that (smooth) maximal surfaces – that is, Riemannian surfaces with vanishing mean curvature in \mathbf{L}^3 – are isothermic surfaces. In [BHS06], the authors showed that there is a special class of S-isothermic nets which corresponds to discrete maximal surfaces (albeit in Euclidean space instead of Lorentz space). This is the advantage of incorporating the theory of incircular nets into discrete differential geometry: it enables us to take known results and apply them to incircular nets. More concretely, since there is a special class of S-isothermic

nets that are discrete maximal surfaces, we identify a special class of isothermic congruences that we call *maximal congruences*. These maximal congruences correspond to discrete maximal surfaces, and therefore we also obtain a special class of incircular isothermic nets that correspond to discrete maximal surfaces. Following [BHS06], discrete maximal surfaces – and therefore maximal incircular nets – are in bijection with hyperbolic orthogonal circle patterns, for which there exists a variational principle which allows one to obtain them uniquely from boundary data [BS04].

In the second part of the paper, we study the associated family f^φ , $\varphi \in \mathbb{S}^1 = [0, 2\pi]$ of a discrete maximal surface f^0 . The associated family of a discrete maximal surfaces was also introduced in [BH16], as an analogue of the associated family of a maximal surface in the smooth setup. Note that each surface f^φ in the associated family is also a maximal surface and is isometric to the initial maximal surface f^0 . We show that the nets f^φ in the associated family of a discrete maximal surface are in 2:1 correspondence with contact congruences. Furthermore, by slightly modifying the way the correspondence works, we are able to show that there is also a 2:1 correspondence of nets f^φ with null congruences. Finally, we show that the X -variables in the associated family are independent of φ . As a result of the correspondence between discrete maximal surfaces and maximal incircular nets, we are also able to construct an associated family of maximal incircular nets.

1.1 Plan of the paper

In Section 2 we recall some important properties of smooth maximal surfaces which motivate the discrete theory. In Section 3 and Section 4 we recall the necessary theory of isothermic congruences and isothermic incircular nets respectively. In Section 5 we explain Koebe congruences, which correspond to the conformal data from which we construct maximal congruences. In Section 6 we recall how to obtain the Christoffel dual, which we use in Section 7 to define maximal congruences from Koebe congruences. This process also allows for a Weierstraß representation as given in Section 8. In Section 9 and Section 10 we investigate the associated family of corresponding S-isothermic nets and null congruences of a maximal congruence. Finally, in Section 11 we show that every member of the associated family defines the same Ising model.

Acknowledgments

N.C. Affolter and N. Smeenk were supported by the Deutsche Forschungsgemeinschaft (DFG) Collaborative Research Center TRR 109 “Discretization in Geometry and Dynamics”. N.C. Affolter was also supported by the ENS-MHI chair funded by MHI. F. Dellinger and C. Müller gratefully acknowledge the support by the Austrian Science Fund (FWF) through grant I 4868 (SFB-Transregio “Discretization in Geometry and Dynamics”) and project F77 (SFB “Advanced Computational Design”) . D. Polly was supported by the French National Agency for Research (ANR) via the grant ANR-18-CE40-0033 (DIMERS) for an inspiring research visit to Paris in the fall of 2021.

N.C. Affolter would like to thank Dmitry Chelkak for pushing for the development of a discrete theory of maximal s-embeddings, as well as him and Misha Bashok and Rémy Mahfouf for countless explanations and discussions of the Lorentz lift. We would also like to thank Jan Techter, Cédric Boutillier, Carl Lutz, Paul Melotti, Sanjay Ramassamy, Marianna Russkikh and Boris Springborn.

2 Smooth maximal surfaces

Before we develop our discrete theory, we give some reminders of results from the smooth theory. These serve as motivation for the discrete setting in the upcoming sections.

An immersed surface in \mathbf{L}^3 is called *spacelike* if the induced metric on its tangent planes is positive definite. For a spacelike immersion, the Gauß map N takes values in the (upper half of the) spacelike unit sphere \mathbf{U}_+ .

We call a spacelike surface *isothermic* if it admits conformal curvature lines. That is, there exists an *isothermic immersion* $f : (u, v) \mapsto f(u, v)$ such that

$$N_u = \kappa_1 f_u, \quad N_v = \kappa_2 f_v, \quad \text{and} \quad \|f_u\|^2 = \|f_v\|^2 =: E,$$

for some functions κ_1, κ_2 , which we call the *principle curvatures*. The *mean curvature* is given by the arithmetic mean of κ_1 and κ_2 .

As in Euclidean space, (spacelike) isothermic surfaces in \mathbf{L}^3 are preserved by (Lorentz) Möbius transformations, in the sense that any Möbius transformation maps isothermic surfaces to isothermic surfaces. Furthermore, they can be characterized by the existence of a certain dual isothermic surface.

Theorem 2.1. *Let $f : U \subset \mathbb{R}^2 \rightarrow \mathbf{L}^3$ be an immersion on an open subset of \mathbb{R}^2 . Then, f is an isothermic immersion if and only if there exists an immersion $f^* : U \rightarrow \mathbf{L}^3$ such that*

$$f_u^* = \frac{f_u}{E}, \quad f_v^* = -\frac{f_v}{E}. \quad (2.1)$$

Moreover, f^* is isothermic and is called the Christoffel dual. ■

A *maximal surface* is a spacelike immersion with vanishing mean curvature. These surfaces maximize local area. They are the natural counterparts of minimal surfaces in Euclidean space and share many of their properties. Most importantly, we have the following facts (see [Pem20]).

Theorem 2.2. *All maximal surfaces are isothermic. A spacelike isothermic immersion is maximal if and only if its Christoffel dual is contained in a spacelike sphere. Furthermore, the Christoffel dual is the Gauß map of the maximal surface (up to scaling and translation).* ■

Theorem 2.2 may be used to derive the Weierstraß representation of maximal surfaces [Kob83, Thm 1.1], based on the observation that the Gauß map N of a maximal surface parametrizes (a part of) the spacelike unit sphere \mathbf{U}_+ isothermically. Moreover, N corresponds to a holomorphic map g via the inverse of the stereographic projection

$$\sigma : \mathbb{C} \rightarrow \mathbf{U}_+ : z \mapsto \frac{1}{1 - |z|^2} \operatorname{Re} \begin{pmatrix} 2z \\ -2iz \\ 1 + |z|^2 \end{pmatrix}.$$

Conversely, any holomorphic map induces the Gauß map of a maximal surface. We can integrate the Christoffel equations (2.1), which recovers the Weierstraß formula

$$f(z) = \operatorname{Re} \int G(\xi) d\xi, \quad (2.2)$$

with

$$G(z) = \frac{1}{g'(z)} \begin{pmatrix} 1 + g^2(z) \\ i(1 - g^2(z)) \\ 2g(z) \end{pmatrix}.$$

Here the surface f is parametrized using the complex coordinate $z = u + iv$. Given the holomorphic function g , Equation (2.2) is a conformal curvature line parametrization of f . All maximal surfaces can be parametrized in this way.

Equation (2.2) can also be used to define the associated family of a minimal surface: given a maximal surface f parametrized as in Equation (2.2), we define its *associated family* f^φ with $\varphi \in \mathbb{S}^1$ via

$$f^\varphi(z) = \operatorname{Re} \int G(\xi) e^{i\varphi} d\xi. \quad (2.3)$$

All members of the associated family of a maximal surface are maximal themselves. Let us give a geometric interpretation of Equation (2.3). The directions of coordinate lines on the maximal surface parametrized by $f = f^0$ are given by $f_u = \operatorname{Re} G$ and $f_v = \operatorname{Im} G$. Moreover, f is a conformal parametrization, which means that f_u and f_v are orthogonal and have equal lengths. The coordinate directions of f^φ are then given by rotating $\operatorname{Re} G$ and $\operatorname{Im} G$ by the angle φ in the tangent plane. Thus, all surfaces in the associated family are parametrized by conformal coordinates, but not necessarily along curvature lines. For $\varphi = \frac{\pi}{2}$ we obtain conformal asymptotic coordinates.

3 Isothermic congruences

Let us discuss the basic geometric objects from the literature that we will need in the remainder of the paper. We consider the bipartition of \mathbb{Z}^2 into black vertices \mathbb{Z}_\bullet^2 and white vertices \mathbb{Z}_\circ^2 , that is

$$\mathbb{Z}_\bullet^2 = \{z \in \mathbb{Z}^2 \mid z_1 + z_2 \in 2\mathbb{Z}\}, \quad \mathbb{Z}_\circ^2 = \{z \in \mathbb{Z}^2 \mid z_1 + z_2 \in 2\mathbb{Z} + 1\}.$$

Note that $\mathbb{Z}_\bullet^2 \simeq \mathbb{Z}_\circ^2 \simeq \mathbb{Z}^2$, therefore we may also speak of black (white) edges which are edges of \mathbb{Z}_\bullet^2 (\mathbb{Z}_\circ^2). There is a natural correspondence between the black edges $E(\mathbb{Z}_\bullet^2)$ and the white edges $E(\mathbb{Z}_\circ^2)$ or the faces $F(\mathbb{Z}^2)$. Similarly, black vertices \mathbb{Z}_\bullet^2 and white faces $F(\mathbb{Z}_\circ^2)$ correspond.

In Lorentz space $\mathbf{L}^3 = \mathbb{R}^{2,1}$, we denote by $\vec{\mathcal{S}}_-(\mathbf{L}^3)$ the set of oriented timelike spheres, by $\mathcal{S}_0(\mathbf{L}^3)$ the set of null-spheres, and by $\vec{\mathcal{L}}_0(\mathbf{L}^3)$ the set of oriented isotropic lines. See [ADM⁺24, Section 3] for a quick introduction to Lorentz sphere geometry.

Definition 3.1. A *null congruence* c is the triple of maps

$$c_\circ : \mathbb{Z}_\circ^2 \rightarrow \vec{\mathcal{S}}_-(\mathbf{L}^3), \quad c_\bullet : \mathbb{Z}_\bullet^2 \rightarrow \mathcal{S}_0(\mathbf{L}^3), \quad c_\square : F(\mathbb{Z}^2) \rightarrow \vec{\mathcal{L}}_0(\mathbf{L}^3),$$

such that the oriented sphere $c(v)$ is in oriented contact with the oriented isotropic line $c_\square(f)$ whenever v and f are incident, see Figure 1. The *center net* (of a null congruence c) is the map $\odot c : \mathbb{Z}^2 \rightarrow \mathbf{L}^3$, such that $\odot c(v)$ is the center of the sphere $c(v)$. ■

Null congruences were introduced as a special case of the so called *contact congruences* in [ADM⁺24]. Note that we wrote that c is the triple of maps $c_\circ, c_\bullet, c_\square$, although technically we treat c as the union of the maps $c_\circ \cup c_\bullet \cup c_\square$ and consequently $c_\circ, c_\bullet, c_\square$ as restrictions of c .

Next, we want to introduce a special class of null congruences, for which we need the classical notion of a (discrete) conjugate net, see [Sau33, DS97, BS08].

Definition 3.2. A map $x : \mathbb{Z}^2 \rightarrow \mathbb{R}^n$ is a *conjugate net* if the image of the vertices of each face $f \in F(\mathbb{Z}^2)$ are contained in a plane. We denote this plane by $x(f)$. ■

Moreover, we call a conjugate net spacelike if all the face-planes are spacelike.

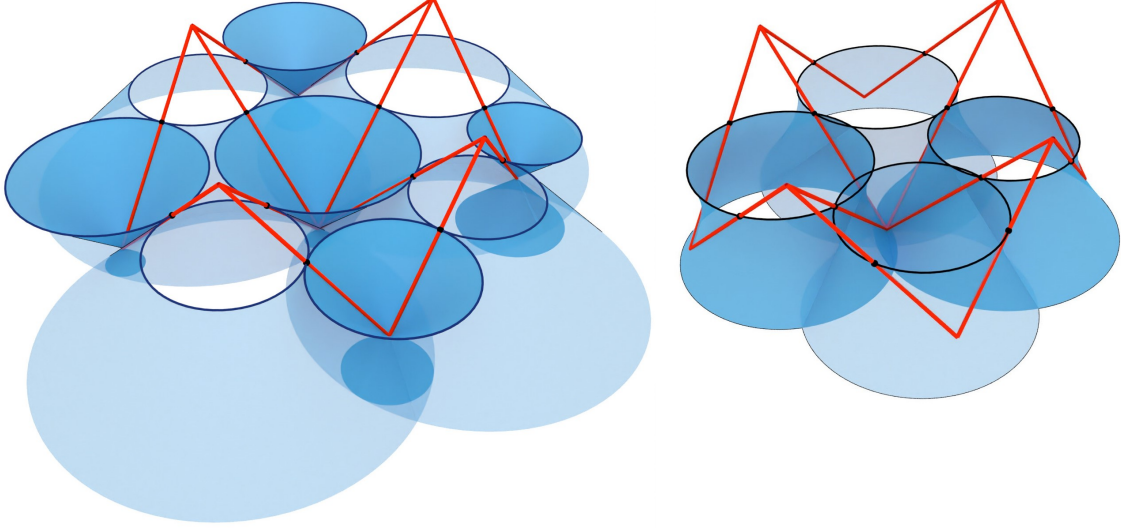


Figure 1: The null-spheres c_\bullet (left) and time-like spheres c_\circ (right) of a null congruence c as well as the isotropic lines c_\square (red).

Definition 3.3. A (spacelike Lorentz) isothermic congruence is a null congruence c such that $\odot c_\circ$ is a spacelike conjugate net. ■

Isothermic congruences were introduced in [ADM⁺24], and are of particular use because they are in correspondence with the following known object from discrete differential geometry. Let us denote by $\mathcal{C}_+(\mathbf{L}^3)$ the set of spacelike circles (which are intersections of spheres with spacelike planes).

Definition 3.4. A (spacelike Lorentz) S-isothermic net h is a collection of maps

$$h_\circ : \mathbb{Z}_\circ^2 \rightarrow \vec{\mathcal{S}}_-(\mathbf{L}^3), \quad h_\bullet : \mathbb{Z}_\bullet^2 \rightarrow \mathcal{C}_+(\mathbf{L}^3), \quad h_\square : F(\mathbb{Z}^2) \rightarrow \mathbf{L}^3,$$

such that for all faces $f = (w, b, w', b') \in F(\mathbb{Z}^2)$ the two spheres $h_\circ(w), h_\circ(w')$ are in oriented contact and the two circles $h_\bullet(b), h_\bullet(b')$ intersect the two spheres orthogonally in the point $h_\square(f)$, see Figure 2 (left). The center net of an S-isothermic net h is the map $\odot h : \mathbb{Z}^2 \rightarrow \mathbf{L}^3$, such that $\odot h(v)$ is the center of $h(v)$ for all $v \in \mathbb{Z}^2$. ■

The original definition of S-isothermic nets was given for Euclidean space [BP99], which was subsequently translated to Lorentz space in [BHS24, ADM⁺24]. The correspondence to isothermic congruences is given in the next theorem, for a proof see [ADM⁺24].

Theorem 3.5. Every isothermic congruence c defines a unique S-isothermic net h such that $c_\circ = h_\circ$, vice versa every S-isothermic h net defines two isothermic congruences c^1, c^2 such that $h_\circ = c_\circ^1 = c_\circ^2$. ■

The circles h_\bullet are obtained from the spheres c_\bullet by intersecting each null-sphere $c_\bullet(b)$ with the spacelike plane spanned by the adjacent centers of c_\circ .

4 Isothermic incircular nets

In [ADM⁺24], we showed how null congruences correspond to incircular nets and how we identify the special case of incircular nets that correspond to isothermic congruences. Let us briefly revisit the definitions and theorems that we use in the remainder of the paper.

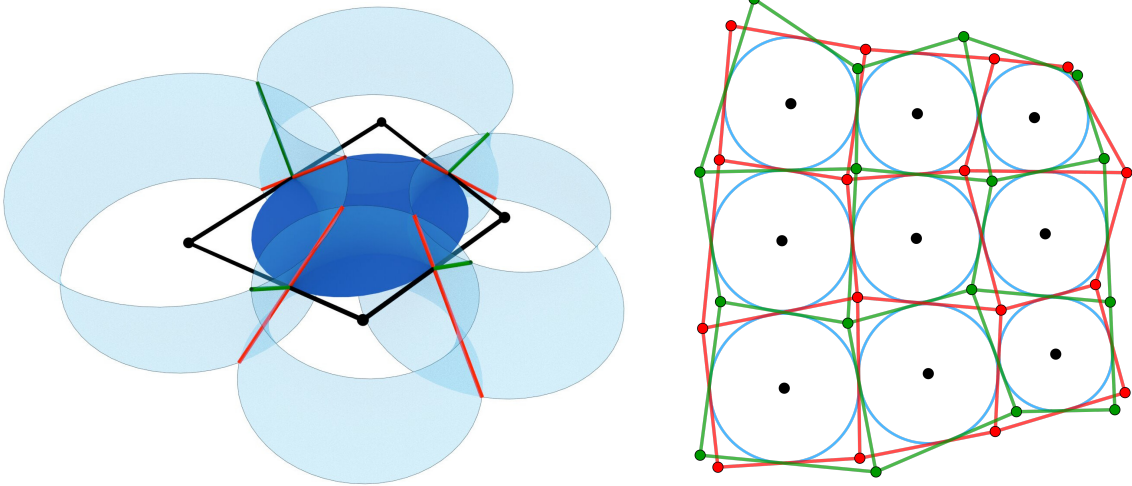


Figure 2: Left: a circle of h_\bullet (blue) of an S-isothermic net h and the four adjacent timelike Lorentz spheres of h_o (teal), as well as the isotropic lines of c_\square^1 (green) and c_\square^2 (red) of the two corresponding isothermic congruences c^1, c^2 . Right: An isothermic incircular net p^1 (green) and the second incircular net p^2 (red) given by the other tangents.

We begin with incircular nets, which are essentially quad nets in \mathbf{E}^2 such that every quad has an incircle, we formalize this in the following definition.

Definition 4.1. An *incircular net* p is a triple of maps

$$p_o : \mathbb{Z}_o^2 \rightarrow \vec{\mathcal{C}}(\mathbf{E}^2), \quad p_\bullet : \mathbb{Z}_\bullet^2 \rightarrow \mathbf{E}^2, \quad p_\square : F(\mathbb{Z}^2) \rightarrow \vec{\mathcal{L}}(\mathbf{E}^2),$$

such that the oriented line $p_\square(f)$ contains $p_\bullet(b)$ and is in oriented contact with $p_o(w)$ whenever $w \in \mathbb{Z}_o^2, b \in \mathbb{Z}_\bullet^2$ are incident with f . ■

Each null congruence c defines an incircular net as follows: For each face f the line $p_\square(f)$ is the orthogonal projection of $c_\square(f)$, $p_\bullet(b)$ is the orthogonal projection of the apex of $c_\bullet(b)$, and $p_o(w)$ is the projection of the smallest circle of $c_o(w)$ (the contour of $c_o(w)$ under orthogonal projection). Every incircular net comes from a null congruence in this way, see [ADM⁺24] for details.

The quantities that define the statistics of the Ising model from an incircular net are the *X-variables* [Che18].

Definition 4.2. Let us identify $\mathbf{E}^2 \simeq \mathbb{C}$ and consider an incircular net p . The *X-variables* $X_o : \mathbb{Z}_o^2 \rightarrow \mathbb{R}$ are defined as

$$X_o(w) = -\frac{(p_\bullet(b_1) - \odot p_o(w))(p_\bullet(b_2) - \odot p_o(w))}{(p_\bullet(b_3) - \odot p_o(w))(p_\bullet(b_4) - \odot p_o(w))},$$

for all $w \in \mathbb{Z}_o^2$ and b_1, b_2, b_3, b_4 adjacent to w in counterclockwise order, with $b_1 = w + (1, 0)$. ■

Note that there is a general definition of *X-variables* for conical nets, in which case the *X-variables* are defined at all vertices of \mathbb{Z}^2 . In the special case of incircular nets, it suffices to consider the *X-variables* at white vertices. The *X-variables* are real because p is a special case of a conical net, see [ADM⁺24, Remark 11.2].

Let c be a null congruence that projects to an incircular net p . Then the *X-variables* of p may also be read off of c as expressed in the next lemma.

Lemma 4.3. *Let c be a null congruence that projects to an incircular net p . Then the X -variables of p satisfy*

$$X_{\circ}(w) = \frac{|\odot c(b_1) - \odot c(b_3)|_{\mathbf{L}^3}^2}{|\odot c(b_2) - \odot c(b_4)|_{\mathbf{L}^3}^2},$$

for all $w \in \mathbb{Z}_{\circ}^2$ and b_1, b_2, b_3, b_4 adjacent to w in counterclockwise order, with $b_1 = w + (1, 0)$. ■

Next, let us characterize which incircular nets are the projections of isothermic congruences. Note that the set of oriented lines that are tangent to two (different) oriented circles in \mathbf{E}^2 has at most two elements. In particular, if the two circles are disjoint as disks then there are exactly two such lines. Thus given one tangent, we may speak of the *other* tangent. If there is only one tangent, then the other tangent refers to the same tangent.

Definition 4.4. *An isothermic incircular net is an incircular net p^1 such that there is a second incircular net p^2 that consists of the other tangents, see Figure 2 (right). ■*

By definition, p^2 is also an isothermic incircular net which has the same incircles as p^1 .

5 Koebe congruences

We briefly revisit circle patterns in the hyperbolic plane. For our purposes the *hyperboloid model* of the hyperbolic plane is particularly practical. Let \mathbf{U}_+ be the (upper half of the) spacelike unit-sphere in \mathbf{L}^3 . We identify the hyperbolic plane \mathcal{H} with \mathbf{U}_+ .

Definition 5.1. *A hyperbolic orthogonal circle pattern q is a pair of maps*

$$q : \mathbb{Z}^2 \rightarrow \mathcal{C}_+(\mathbf{U}_+), \quad q_{\square} : F(\mathbb{Z}^2) \rightarrow \mathbf{U}_+,$$

such that

- (i) around each face f the four circles intersect in the point $q(f)$, and
- (ii) adjacent circles intersect orthogonally. ■

Each circle $q(v)$ in the hyperbolic plane corresponds to the intersection of \mathbf{U}_+ with a plane, and each such plane is in bijection with the polar point $q^{\perp}(v)$ outside of \mathbf{U}_+ . The point $q^{\perp}(v)$ is the center of a (unique) timelike sphere $S(v)$ that intersects \mathbf{U}_+ orthogonally in the circle $q(v)$. This allows us to define an S-isothermic net h by

$$h_{\circ}(w) = S(w), \quad h_{\bullet}(b) = q(b), \quad h_{\square}(f) = q_{\square}(f),$$

We may choose the orientation of one initial sphere of h freely, which then determines the orientations of all other spheres. This motivates the following definition.

Definition 5.2. *A Koebe isothermic net is an S-isothermic net h such that every circle of h_{\bullet} is contained in the upper half of the unit-sphere \mathbf{U}_+ , see Figure 4 (left). A Koebe congruence is an isothermic congruence that corresponds to a Koebe isothermic net via Theorem 3.5. ■*

It is not hard to see that Koebe isothermic nets are exactly those isothermic nets that correspond to hyperbolic orthogonal circle patterns. An advantage of hyperbolic orthogonal circle patterns (and therefore Koebe isothermic nets) is that they can be constructed from boundary data as the minimizer of a certain convex functional, see [BS04]. In fact, existence and uniqueness is guaranteed, and this also works for combinatorics that are more general than \mathbb{Z}^2 .

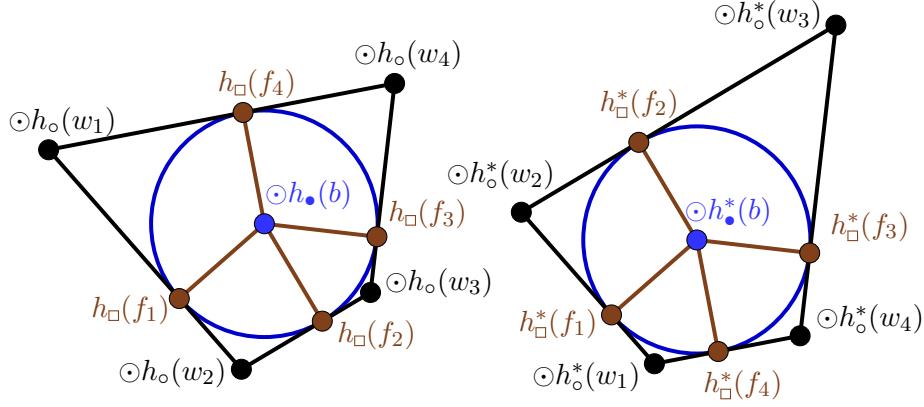


Figure 3: Local Christoffel dual h^* of an S-isothermic net h . Corresponding edges (black and brown) are parallel.

Remark 5.3. Let h be a Koebe isothermic net. At each face f there is a unique tangent $T(f)$ to the two adjacent circles of h_\bullet , which is also a tangent to \mathbf{U}_+ . Around a white vertex w , the adjacent tangents intersect in the point $\odot h_\circ(w)$. Viewed in this way, as an edge-tangent conjugate net, $\odot h_\circ$ is called a *Koebe polyhedron* [BS04, BHS06]. Note that after a projective transformation, $\odot h_\circ$ is still a Koebe polyhedron, edge-tangent to a new quadric which is the image of \mathbf{U}_+ . In particular, there are projective transformations that map \mathbf{U}_+ to $\mathbb{S}^2 \subset \mathbb{R}^3$. There are also projective transformations that fix \mathbf{U}_+ or fix \mathbb{S}^2 , which are the corresponding Möbius transformations of \mathbf{U}_+ or \mathbb{S}^2 , respectively. In particular, this enables us to start with a Euclidean Koebe polyhedron and map it to a Lorentz Koebe polyhedron that is edge tangent to only the upper half of \mathbf{U}_+ . Thus, the difference between treating Lorentz maximal surfaces and Euclidean minimal surfaces lies only in the treatment of the boundary conditions, which are given in the hyperbolic plane \mathcal{H}^2 or the Euclidean plane \mathbf{E}^2 , respectively. ■

Remark 5.4. Which isothermic incircular nets are projections of Koebe congruences? Recall that isothermic incircular nets come in pairs p^1, p^2 (Definition 4.4) which share the same incircles. For every black vertex $b \in \mathbb{Z}_\bullet^2$ we may define the line $\ell(b)$ spanned by $p_\bullet^1(b)$ and $p_\bullet^2(b)$. An isothermic incircular net comes from a Koebe congruence if and only if all the lines $\ell(b)$ intersect in a point. This can be shown by observing that each line $\ell(b)$ is the projection of the axis of the corresponding circle h_\bullet in the Koebe isothermic net h . If the axes all intersect in a point, this point is the center of the unit-sphere \mathbf{U}_+ . Also note that if all the lines are parallel or are all points (in the degenerate case that $p^1 = p^2$), then the circles of h are all contained in a plane. Thus h is essentially flat and is not a Koebe congruence. ■

6 Christoffel dual

Let us briefly recall the *Christoffel dual* for S-isothermic nets [BHS06] with the notation as in [ADM⁺24], see also Figure 3. Let us denote by

$$h_{\boxplus} = \odot h \cup h_{\square} : \mathbb{Z}^2 \simeq (\mathbb{Z}^2 \cup F(\mathbb{Z}^2)) \rightarrow \mathbf{L}^3, \quad (6.1)$$

the combination of center net $\odot h$ and contact points h_{\square} of an S-isothermic net h , defined on $\mathbb{Z}^2 \cup F(\mathbb{Z}^2)$, which we identify with \mathbb{Z}^2 for the time being. In this notation, we define the discrete differential

$$dh_{\boxplus}(v, v') = h_{\boxplus}(v') - h_{\boxplus}(v),$$

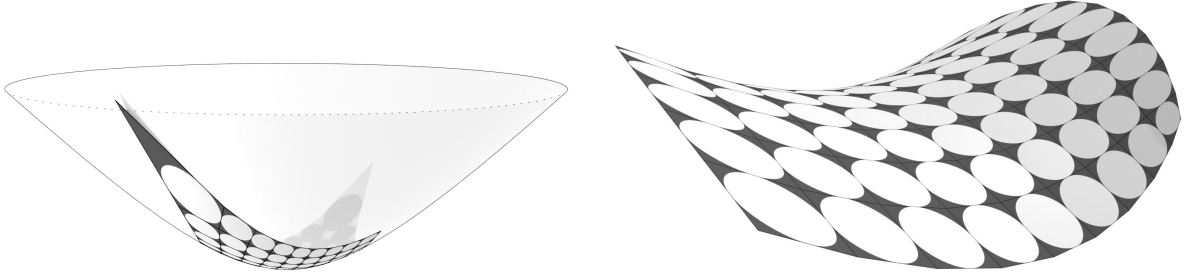


Figure 4: Left: the circles of a Koebe isothermic net. Right: the circles of a discrete maximal surface.

for all adjacent $v, v' \in \mathbb{Z}^2$. We also define the dual differential

$$dh_{\boxplus}^*(v, v') = \pm \frac{dh_{\boxplus}(v', v)}{|dh_{\boxplus}(v', v)|^2},$$

for all adjacent $v, v' \in \mathbb{Z}^2$, where the sign is $+$ if the edge (v, v') is horizontal or $-$ if the edge is vertical in \mathbb{Z}^2 . This dual form is *closed*, which means it may be integrated to obtain a map $h_{\boxplus}^* : \mathbb{Z}^2 \rightarrow \mathbf{L}^3$. In fact, it can be shown that h_{\boxplus}^* defines a unique S-isothermic net h^* (up to translation), which is called the *Christoffel dual* of h .

The identification in Theorem 3.5 implies that there is also a sensible definition of the Christoffel dual c^* of an isothermic congruence c . Consider the combined map

$$c_{\boxplus} = \odot c \cup h_{\square} : \mathbb{Z}^2 \simeq V(\mathbb{Z}^2) \cup F(\mathbb{Z}^2) \rightarrow \mathbf{L}^3,$$

that is the combination of $\odot c$ and h_{\square} . In comparison with h_{\boxplus} we substituted $\odot h_{\bullet}$ with $\odot c_{\bullet}$, therefore c_{\boxplus} is not a conjugate net. However, for a face f and an adjacent white vertex w or black vertex b it is possible to integrate

$$dc_{\boxplus}^*(f, w) = \pm \frac{dc_{\boxplus}(f, w)}{R(w)^2}, \quad dc_{\boxplus}^*(f, b) = \pm \frac{dc_{\boxplus}(f, b)}{r(b)^2}, \quad (6.2)$$

where $R(w)$ is the radius of $h_{\square}(w)$ and $r(b)$ is the radius of the incircle of the corresponding quad of $\odot c_{\square}$ at b . The difference to the formula for dh_{\boxplus}^* is that we cannot divide by $|dc_{\boxplus}(f, b)|$, since that length is zero. Instead, this formula works since the triangle $h_{\square}(f), \odot h_{\bullet}(b), \odot c_{\bullet}(b)$ is a right-angled triangle and

$$|h_{\square}(f) - \odot h_{\bullet}(b)|^2 = -|\odot h_{\bullet}(b) - \odot c_{\bullet}(b)|^2.$$

The discrete differential dc_{\boxplus}^* is consistent in the sense that the integrated net c_{\boxplus}^* is indeed the combination of $\odot c^*$ and h_{\square}^* .

7 Maximal surfaces

Definition 7.1. A (*discrete spacelike Lorentz*) *maximal surface* is an S-isothermic net h such that the Christoffel dual h^* is a Koebe isothermic net (see Figure 4). A (*spacelike Lorentz*) *maximal congruence* is an isothermic congruence c such that the Christoffel dual congruence c^* is a Koebe congruence. \blacksquare

The following direct characterization of discrete maximal surfaces is an immediate translation of the characterization of discrete minimal surfaces in [BHS06, Definition 6].

Theorem 7.2. *An S -isothermic net h is a maximal surface if and only if for each white vertex w and its four adjacent vertices b_1, b_2, b_3, b_4 the four circle centers $\odot h_\bullet(b_1), \odot h_\bullet(b_2), \odot h_\bullet(b_3), \odot h_\bullet(b_4)$ are contained in a plane. \blacksquare*

If c is a maximal congruence, we understand the Koebe congruence c^* as the normal map of c , in the sense that the vectors from the origin (the center of the unit-sphere \mathbf{U}_+) to each point $\odot c_\circ^*(w)$ are the normal vectors at $\odot c_\circ(w)$.

Let $t \in \mathbb{R}$ and consider the map

$$\odot c_\circ^t = \odot c_\circ + t \odot c_\circ^*.$$

We think of $\odot c_\circ^t$ as an *offset surface* of $\odot c_\circ$, since it is edge- (and face-) parallel to $\odot c_\circ$ at some offset distance t . Each face of $\odot c_\circ^t$ has an area A^t that changes quadratically in t . This change is captured by the (*discrete*) *Steiner formula* [Sch03, Sch06, LPW⁺06, BPW10, BS08]

$$A^t = A^0 - 2Ht + Kt^2,$$

where we understand H as the (*discrete*) *mean curvature* and K as the (*discrete*) *Gauß curvature*. Because $\odot c_\circ$ is a Koenigs net (see [ADM⁺24, BS08]), a simple computation shows that H is actually *zero*. This provides another justification for calling maximal congruences maximal, since they have constant discrete mean curvature zero, compare with Section 2.

Remark 7.3. Which isothermic incircular nets are projections of maximal congruences? Let us give a local characterization which uses four black vertices b_1, b_2, b_3, b_4 adjacent to a white vertex w in circular order. Consider the lines $\ell(b_1), \ell(b_2), \ell(b_3), \ell(b_4)$ as in Remark 5.4, as well as the four intersection points $P_{12}, P_{23}, P_{34}, P_{41}$ given by consecutive lines – that is, $P_{12} = \ell(b_1) \cap \ell(b_2)$ and so on. Let us also denote by $M_i = \frac{1}{2}(p^1(b_i) + p^2(b_i))$ the midpoint of the two corresponding points in the pair of isothermic incircular nets p^1, p^2 , which is on $\ell(b_i)$. Then p^1, p^2 are the projection of a maximal congruence if and only if

$$\frac{M_1 - P_1}{P_1 - M_2} \frac{M_2 - P_2}{P_2 - M_3} \frac{M_3 - P_3}{P_3 - M_4} \frac{M_4 - P_4}{P_4 - M_1} = 1,$$

where we evaluate the equation by identifying \mathbf{E}^2 with the complex plane \mathbb{C} . The equation is a generalization of Menelaus' theorem (see [BS08]) that characterizes the observation in Theorem 7.2, that is, the coplanarity of the four circle centers $h(b_i)$. \blacksquare

8 Weierstraß representation

The geometric idea of the *discrete Weierstraß representation* is as follows. First of all, we understand an orthogonal circle pattern in \mathbb{R}^2 as a discrete conformal map [Sch97]. If restricted to the unit disc, the orthogonal circle pattern is a hyperbolic orthogonal circle pattern in the Poincaré disk model of the hyperbolic plane. Then, we lift the orthogonal circle pattern via inverse stereographic projection to the upper half of the timelike unit-sphere \mathbf{U}_+ to obtain a hyperbolic orthogonal circle pattern in \mathbf{U}_+ (as in Definition 5.1). Then we take the Christoffel dual to obtain the corresponding discrete maximal surface. Each operation may be expressed via formulas, combining them all yields the discrete Weierstraß representation, analogous to the smooth setting (see Section 2).

Compared to the discrete Weierstraß representation for minimal surfaces in Euclidean space [BHS06], we only need to adapt some of the signs in the formula to the Lorentz setup. Let q be a hyperbolic orthogonal circle pattern in the Poincaré disk model, that is, in the unit-disk in $\mathbb{R}^2 \simeq \mathbb{C}$. The points $q_\square : F(\mathbb{Z}^2) \rightarrow \mathcal{H}^2$ are the intersection points of q which are contained

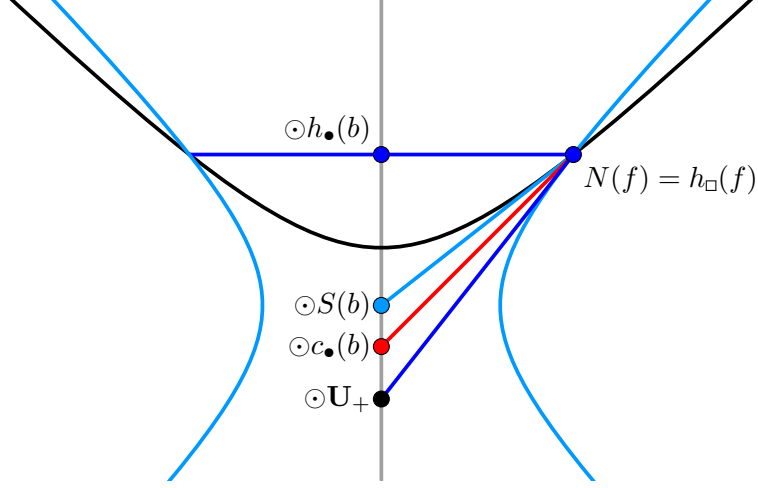


Figure 5: Local configuration in a Koebe isothermic net h and the corresponding null congruence c . We see the unit-sphere \mathbf{U}_+ (black), the circle $h(b)$ and the normal vector $N(f) = h_\square(f)$ (dark blue), the sphere $S(b)$ and its center $\odot S(b)$ (teal), and finally the center of the null-sphere $c_\bullet(b)$ as well as its generator containing $h_\square(f)$ (red).

in the unit disk $\mathcal{H}^2 \subset \mathbb{C}$. Let us also denote by $\rho(v)$ the radius and by $\odot q(v)$ the center of the circle $q(v)$. Let h be the Koebe isothermic net that stereographically projects to q , and h^* the corresponding maximal surface. Let w, w' be two white vertices adjacent to a common face f . Then

$$\odot h_\circ^*(w) - \odot h_\circ^*(w') = \pm \operatorname{Re} \left[\frac{R_\circ^*(w) + R_\circ^*(w')}{1 - |q_\square(f)|^2} \frac{\overline{\odot q_\circ(w)} - \overline{\odot q_\circ(w')}}{|\odot q_\circ(w) - \odot q_\circ(w')|} \begin{pmatrix} 1 + |q_\square(f)|^2 \\ i(1 - |q_\square(f)|^2) \\ 2q_\square(f) \end{pmatrix} \right], \quad (8.1)$$

where R_\circ^* are the radii of the spheres of h_\circ^* , which may be expressed as

$$R_\circ^*(w) = \frac{1 - |\odot q_\circ(w)|^2 + \rho_\circ(w)^2}{2\rho_\circ(w)}. \quad (8.2)$$

Now, let c^* be one of the two null congruences that correspond to h^* , as in Theorem 3.5. Additionally, let p^* be the incircular net corresponding to c^* . We may restrict Equation (8.1) to the first two coordinates to obtain an explicit differential formula for $\odot p_\circ^*$. Thus, we know the incircle centers of p^* . Moreover, the incircle radii (the radii of p_\circ^*) are simply the radii R_\circ^* . Hence, the incircles p_\circ^* are determined. By taking the tangents p_\square^* to the incircles in a consistent manner, we also obtain the whole of p_\square^* , and therefore also p_\bullet^* .

However, the main advantage of the Weierstraß representation is to have explicit formulas. Therefore, we now briefly explain how to obtain explicit formulas not just for p_\circ^* but also for p_\bullet^* .

First, note that since h is a Koebe isothermic net there is also a sphere $S(b)$ that intersects \mathbf{U}_+ orthogonally in the circle $h_\bullet(b)$, see Figure 5. The goal is to calculate $\odot c_\bullet^*(b) - h_\square^*(f)$ for incident $b \in \mathbb{Z}_\bullet^2$, $f \in F(\mathbb{Z}^2)$, which we do by using Equation (6.2) which shows that

$$\odot c_\bullet^*(b) - h_\square^*(f) = \frac{\odot c_\bullet(b) - h_\square(f)}{r_\bullet(b)^2}.$$

Here, $r_\bullet(b)$, the radius of the circle $h_\bullet(b)$, may be calculated by three instances of Pythagoras' theorem in Figure 5. This yields

$$r_\bullet(b) = \frac{R_\bullet(b)}{\sqrt{1 - R_\bullet(b)^2}},$$

where $R_{\bullet}(b)$ is the radius of $S(b)$ which is expressed, analogously to Equation (8.2), as

$$R_{\bullet}(w) = \frac{2\rho_{\bullet}(w)}{1 - |\odot q_{\bullet}(w)|^2 + \rho_{\bullet}(w)^2}. \quad (8.3)$$

Thus, it remains to calculate $\odot c_{\bullet}(b) - h_{\square}(f)$. The point of contact $h_{\square}(f)$ an *edge normal* of both h and h^* , which is why we denote $h_{\square}(f)$ by $N(f)$ for the following computations. The normal $N(f)$ is obtained by stereographic projection, that is

$$N(f) = \operatorname{Re} \left[\frac{1}{1 - |q_{\square}(f)|^2} \begin{pmatrix} 2q_{\square}(f) \\ -i2q_{\square}(f) \\ 1 + |q_{\square}(f)|^2 \end{pmatrix} \right].$$

Additionally, let b' be the other black vertex adjacent to f . We can write

$$\odot S(b) - N(f) = R_{\bullet}(b)T_{\bullet}(f),$$

with

$$T_{\bullet}(f) = \operatorname{Re} \left[\frac{1}{1 - |q_{\square}(f)|^2} \frac{\overline{\odot q_{\bullet}(b)} - \overline{\odot q_{\bullet}(b')}}{|\odot q_{\bullet}(b) - \odot q_{\bullet}(b')|} \begin{pmatrix} 1 + |q_{\square}(f)|^2 \\ i(1 - |q_{\square}(f)|^2) \\ 2q_{\square}(f) \end{pmatrix} \right], \quad (8.4)$$

analogously to Equation (8.1). Moreover, a small calculation shows that

$$\odot c_{\bullet}(b) = \frac{1}{1 \pm R_{\bullet}(b)} \odot S(b) = \frac{1}{1 \pm R_{\bullet}(b)} (N(f) + R_{\bullet}(b)T_{\bullet}(f)).$$

Thus, we are able to write

$$\odot c_{\bullet}(b) - h_{\square}(f) = \frac{R_{\bullet}(b)}{1 \pm R_{\bullet}(b)} (T_{\bullet}(f) \mp N(f)),$$

and therefore, using Equation (8.3),

$$\odot c_{\bullet}^*(b) - h_{\square}^*(f) = \frac{1 \mp R_{\bullet}(b)}{R_{\bullet}(b)} (T_{\bullet}(f) \mp N(f)). \quad (8.5)$$

Furthermore, we have that, where $T_{\circ}(f)$ is obtained analogously to Equation (8.4) as

$$\odot h_{\circ}^*(w) - h_{\square}^*(f) = \pm R_{\circ}^*(w)T_{\circ}(f). \quad (8.6)$$

In conclusion, we are able to obtain combined integral formulas for

- (i) $\odot c_{\circ}^*$, h_{\square} and $\odot c_{\bullet}^*$ (using Equation (8.5) and Equation (8.6)),
- (ii) all of c_{\circ}^* and c_{\bullet}^* (as we have formulas for the radii of these spheres),
- (iii) $\odot p_{\circ}^*$ and $\odot p_{\bullet}^*$ (via projection of our formulas to the first two coordinates),
- (iv) the incircular net p^* in terms of the hyperbolic orthogonal circle pattern q .

9 The associated family

As discussed in Section 2, a smooth maximal surface f comes with an associated family $(f^{\varphi})_{\varphi \in \mathbb{S}^1}$ of maximal surfaces. Each member f^{φ} of the associated family is obtained by rotating df by φ around the surface normal and then integrating the rotated df . In [BHS06] the authors introduce an analogous discrete construction for minimal S-isothermic surfaces in Euclidean space. In this

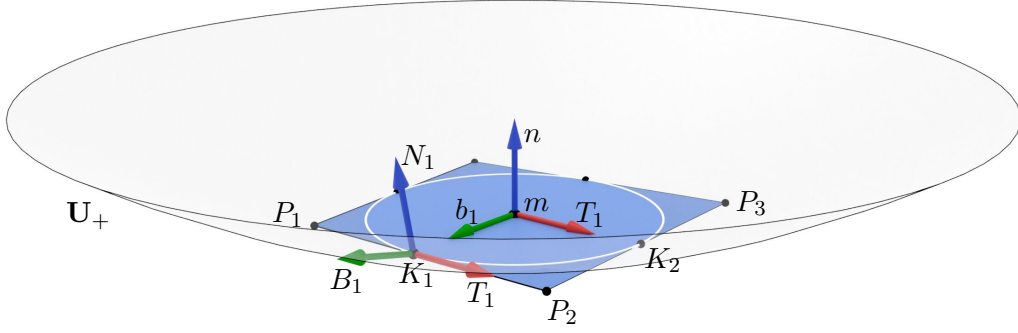


Figure 6: The frames (T_i, n, b_i) and (T_i, N_i, B_i) used in the calculations for the associated family.

section we study how the discrete construction translates to maximal congruences in Lorentz space and the corresponding incircular nets in \mathbf{E}^2 .

Let c be a Koebe congruence and h the corresponding S-isothermic net, and let h_{\boxplus} be the combination of h and h_{\square} as in Equation (6.1). Fix an angle $\varphi \in \mathbb{S}^1$. For a face f , let $J_{\varphi}(f)$ be the (elliptic) Lorentz rotation with angle φ around the (timelike) axis spanned by the center of \mathbf{U}_+ and $h_{\square}(f)$. Define the associated dual differential via

$$d\odot h_{\circ}^{\varphi}(w, w') = \pm(R^{-1}(w) + R^{-1}(w')) \frac{J_{\varphi}(f)[d\odot h_{\circ}(w, w')]}{|d\odot h_{\circ}(w, w')|},$$

for all white vertices w, w' adjacent to the common face f .

Let us investigate the properties of $d\odot h_{\circ}^{\varphi}$ with some calculations. To simplify notation, let $P = (P_1, P_2, P_3, P_4)$ be a planar quad tangential to the space-like unit-sphere \mathbf{U}_+ (like the quads in $\odot h_{\circ}$ of a Koebe congruence). Let T_1, T_2, T_3, T_4 be the unit edge vectors (or unit tangent vectors) of the quad P . Also let R_i be the radii of the spheres at the vertices, so that

$$P_{i+1} - P_i = (R_{i+1} + R_i)T_i.$$

Let K_i be the touching point on the edge $P_i P_{i+1}$, so that $K_i - P_i = R_i T_i$. Also let n be the normal vector of the incircle C with center m and radius r , which passes through the four points K_i . Let $b_i = T_i \times n$ be the (bi)normal vector to T_i in the quad plane, so that $m - K_i = r b_i$.

Recall that the dual quad P^* is defined by

$$P_{i+1}^* - P_i^* = \pm(R_{i+1}^{-1} + R_i^{-1})T_i = (R_{i+1}^* + R_i^*)T_i^*,$$

where $R_i^* = R_i^{-1}$, $T_i^* = \pm T_i$ and the sign is $+$ for horizontal edges and $-$ for vertical edges. The dual contact points satisfy $K_i^* - P_i^* = R_i^* T_i^*$, and the dual incircle radius is $r^* = r^{-1}$. Note that if γ_i is the corner angle at P_i , then in the dual quad we have $\gamma_i^* = \pi - \gamma_i$.

In order to obtain the associated family, let us also consider at each point K_i the normal vector to \mathbf{U}_+ , which we denote by N_i . Note that K_i coincides with N_i by construction, but this will not be the case in the associated family so we use different symbols. To express N_i and $B_i := T_i \times N_i$, we use the rotation matrix in the orthonormal basis (T_i, n, b_i)

$$M_{\theta} = \begin{pmatrix} 1 & 0 & 0 \\ 0 & \cosh \theta & \sinh \theta \\ 0 & \sinh \theta & \cosh \theta \end{pmatrix},$$

so that

$$\begin{aligned} T_i &= M_\theta T_i = T_i, \\ N_i &= M_\theta n = n \cosh \theta + b_i \sinh \theta, \\ B_i &= M_\theta b_i = n \sinh \theta + b_i \cosh \theta. \end{aligned}$$

Following [BHS06], rotation in the associated family means rotating T_i around N_i by an angle φ . In the orthonormal basis (T_i, N_i, B_i) the corresponding rotation matrix is

$$M_\varphi = \begin{pmatrix} \cos \varphi & 0 & -\sin \varphi \\ 0 & 1 & 0 \\ \sin \varphi & 0 & \cos \varphi \end{pmatrix},$$

so that

$$T_i^\varphi = M_\varphi T_i = T_i \cos \varphi + B_i \sin \varphi = T_i \cos \varphi + n \sinh \theta \sin \varphi + b_i \cosh \theta \sin \varphi, \quad (9.1)$$

$$N_i^\varphi = M_\varphi N_i = N_i = n \cosh \theta + b_i \sinh \theta, \quad (9.2)$$

$$B_i^\varphi = M_\varphi B_i = -T_i \sin \varphi + B_i \cos \varphi = -T_i \sin \varphi + n \sinh \theta \cos \varphi + b_i \cosh \theta \cos \varphi. \quad (9.3)$$

The associated quad P^φ is obtained by integrating

$$P_{i+1}^\varphi - P_i^\varphi = \pm(R_{i+1}^* + R_i^*)T_i^\varphi. \quad (9.4)$$

This formula closes in the T_i components since it closes for $\pm T_i = T_i^*$ already, for the n components it is just a telescopic sum, and for the b_i component it follows from the T_i components and the linearity of $b_i = T_i \times n$. Let us put this in a theorem.

Theorem 9.1. *The associated discrete differential $d\odot h_\circ^\varphi$ is closed.* ■

Proof. It suffices to check the closing condition around each black vertex, which corresponds to the fact that P^φ is well-defined in the calculation above. □

Therefore we may integrate $d\odot h_\circ^\varphi$ to obtain a net $\odot h_\circ^\varphi$, which we consider to be a surface in the associated family of $\odot h_\circ^*$. As we will see in the next section, $\odot h_\circ^\varphi$ shares many properties with S-isothermic nets, but not all, and is therefore not an S-isothermic net. Instead, we consider $\odot h_\circ^\varphi$ to be a discrete maximal surface that is still conformally parametrized – but *not* along curvature lines. Thus, we think of $\odot h_\circ^\varphi$ as a discretization of an isothermic surface but not as a discretization of a curvature-line parametrization.

10 The associated congruences

Before we begin, let us recall the notion of a contact congruences [ADM⁺24] which generalizes null-congruences (Definition 3.1) and which we need in the following.

Definition 10.1. A *contact congruence* c is a pair of maps

$$c : \mathbb{Z}^2 \rightarrow \vec{\mathcal{S}}_-(\mathbf{L}^3) \cup \mathcal{S}_0(\mathbf{L}^3), \quad c_\square : F(\mathbb{Z}^2) \rightarrow \vec{\mathcal{L}}_0(\mathbf{L}^3),$$

such that the oriented sphere $c(v)$ is in oriented contact with the oriented isotropic line $c_\square(f)$ whenever v and f are incident. ■

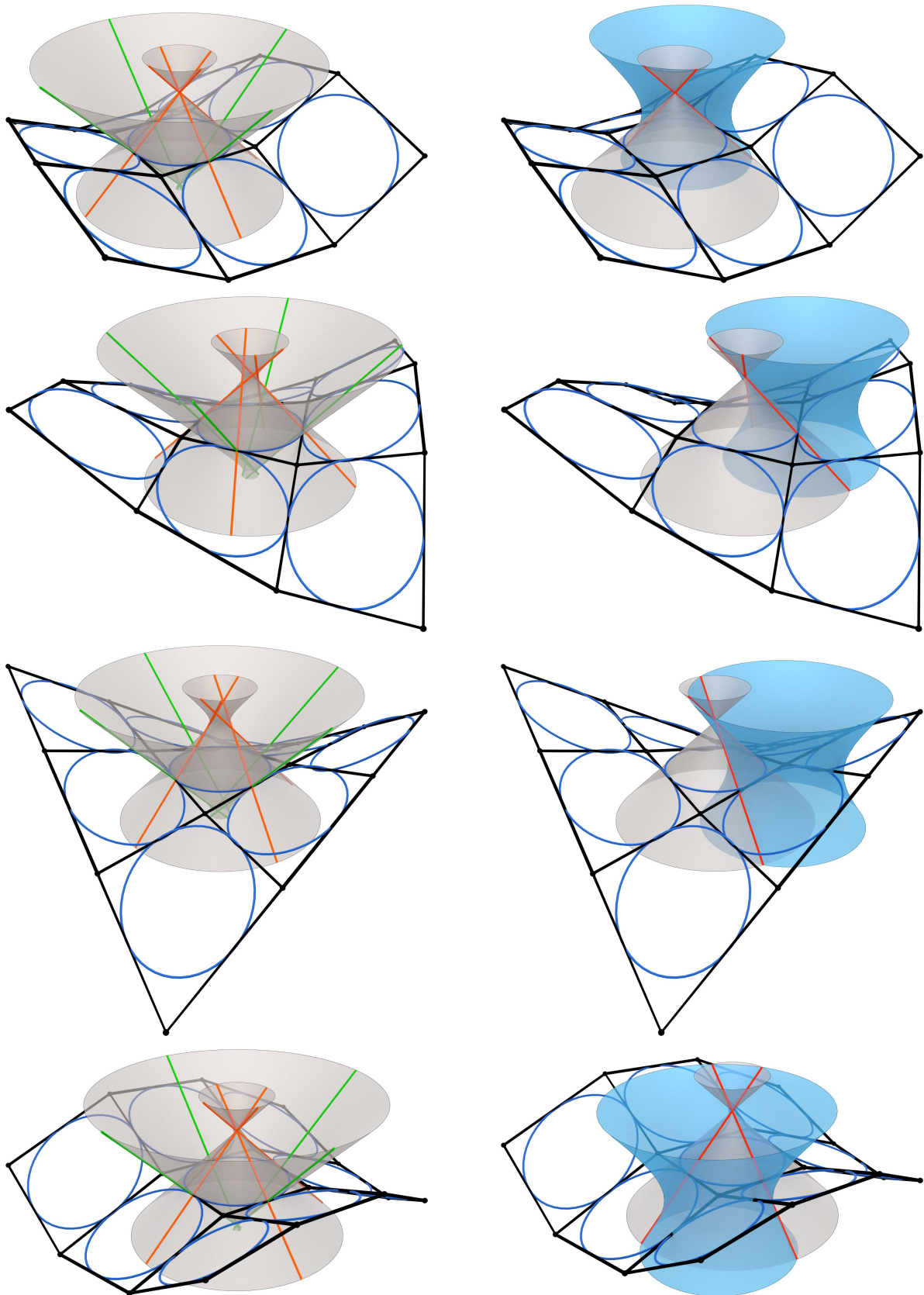


Figure 7: Congruences in the associated family of a maximal surface, from top to bottom for the values $\varphi = 0, \frac{\pi}{4}, \frac{\pi}{2}, \pi$, the latter is a rotation of the original surface. Left: Spheres of the contact congruences $(c^1)^\varphi$ and $(c^2)^\varphi$ of radii $\sin \varphi$. The spheres contain adjacent generators and corresponding face circles. Right: A null sphere and a timelike vertex sphere of one of the associated null congruences \dot{c}^φ .

In the previous section, we followed the technique of [BHS06] translated to Lorentz geometry – with a few more details. In the following we take the calculations further to prove some new results (which do not readily translate from or to Euclidean geometry).

Since a quad $P_1^\varphi, P_2^\varphi, P_3^\varphi, P_4^\varphi$ is obtained by integrating as in Equation (9.4), there are still spheres h_\circ^φ at the white vertices with radii given by $R_i^\varphi = R_i^* = R_i^{-1}$. Moreover, for adjacent white vertices the spheres are touching. Consequently, the touching coins lemma [BHS06] implies that there is still a circle C^φ which passes through the four points of contact $K_1^\varphi, K_2^\varphi, K_3^\varphi, K_4^\varphi$. However, circles of adjacent faces are not touching.

Let us consider the orthogonal projection Q^φ of the quad P^φ to the plane of the circle C^φ .

Lemma 10.2. *The projected quad Q^φ is (Lorentz) similar to P^* , and the scaling factor is $\mu = \sqrt{1 + r^2 \sin^2 \varphi}$. ■*

Proof. Projecting the rotated vectors P^φ onto the plane of C^φ gives a scaled and rotated image of P^* . However, the scaling and rotation only depend on the angles φ and $\theta = \angle(N_i, n)$. These angles are the same for all edges of Q^φ . Hence, the quad Q^φ is similar to P^* . The scaling factor can be derived from the quotient of lengths of the orthogonal projection of T^φ denoted by U^φ and T^φ . We obtain from Equation (9.1) that

$$U_i^\varphi = T_i \cos \varphi + b_i \cosh \theta \sin \varphi.$$

Consequently,

$$\mu = |U_i^\varphi| = \sqrt{\cos^2 \varphi + \cosh^2 \theta \sin^2 \varphi} = \sqrt{1 + r^2 \sin^2 \varphi},$$

is the scaling factor of the edge lengths (we used that $\sinh \theta = r$). □

As a consequence of Lemma 10.2, the quad Q^φ has an incircle D^φ with radius μr^* , and center m^φ which coincides with the center of C^φ .

As mentioned above, the spheres centered at P_i^φ and P_{i+1}^φ still touch in K_i^φ . Let us call the two common isotropic lines of these spheres $G_{i,\pm}^\varphi$.

Lemma 10.3. *The four isotropic lines $G_{1,+}^\varphi, G_{2,-}^\varphi, G_{3,+}^\varphi, G_{4,-}^\varphi$ are contained in a sphere of radius $\rho_\varphi := \sin \varphi$. The four isotropic lines $G_{1,-}^\varphi, G_{2,+}^\varphi, G_{3,-}^\varphi, G_{4,+}^\varphi$ are also contained in a (generically different) sphere of radius ρ_φ , see Figure 7 (left). ■*

Proof. Note that $G_{i,\pm}^\varphi$ are both orthogonal to T_i^φ . Thus, the direction vectors of the two isotropic lines are given by

$$N_i^\varphi \pm B_i^\varphi = \mp T_i \sin \varphi + n(\cosh \theta \pm \sinh \theta \cos \varphi) + b_i(\sinh \theta \pm \cosh \theta \cos \varphi).$$

The projection of the line $G_{i,\pm}^\varphi$ to the plane of the circle C^φ is a line that has distance ρ^φ to the center m^φ , where

$$\begin{aligned} \rho^\varphi &= \mu r^* \left\langle \underbrace{\frac{-T_i \cosh \theta \sin \varphi + b_i \cos \varphi}{\mu}}_{\text{normal to } U_i^\varphi}, \underbrace{\frac{T_i(-\sinh \theta \mp \cosh \theta \cos \varphi) \mp b_i \sin \varphi}{\sqrt{\sin^2 \varphi + (\sinh \theta \pm \cosh \theta \cos \varphi)^2}}}_{\text{normal of projected } G_{i,\pm}^\varphi} \right\rangle \\ &= \frac{r^* \sinh \theta (\cosh \theta \pm \sinh \theta \cos \varphi) \sin \varphi}{\sqrt{(\cosh \theta \pm \sinh \theta \cos \varphi)^2}} = r^* \sinh \theta \sin \varphi = \sin \varphi, \end{aligned}$$

(independently of i), since $\sinh \theta = r$ and $rr^* = 1$. Because the lines $G_{i,\pm}^\varphi$ are isotropic, ρ^φ is also the distance of $G_{i,\pm}^\varphi$ to the axis of C^φ . As the lines are also the same distance of the center of C^φ , there are two unique Lorentz spheres of radii ρ^φ containing the quadruples of isotropic

lines of the lemma. The circle C^φ is contained in both spheres. Note that this is not the smallest Euclidean circle of the spheres. The change of sign of the generators in one sphere is due to the change of orientation of vertical edges when dualizing. \square

Surprisingly, ρ^φ does not depend on r or (equivalently) on θ . Hence, the radii ρ^φ are the same for all quads in the associated surface.

By combining the generalization of null congruences to contact congruences (Definition 10.1) with Lemma 10.3, we obtain the following theorem.

Theorem 10.4. *Let h be a Koebe net and h^φ a member of the associated family of h^* (the Christoffel dual S-maximal surface). Then there are two contact congruences $(c^1)^\varphi$, $(c^2)^\varphi$ such that $(c^1_\circ)^\varphi = (c^2_\circ)^\varphi = h^\varphi_\circ$, which we call associated congruences. \blacksquare*

Proof. By Lemma 10.3, for each black vertex b there are exactly two spheres per face that are in oriented contact with the four spheres $h^\varphi_\circ(w_i)$ of adjacent white vertices w_i . Choosing one of the two spheres for some black vertex b_0 and then all other spheres consistently proves the claim. \square

Additionally, it is possible to define a new contact congruence \dot{c} such that $\odot\dot{c} = \odot c$, and such that the radii of all spheres of \dot{c}_\bullet are zero, while at white vertices the radii satisfy

$$\dot{R}(v) = R(v) - \rho_\varphi. \quad (10.1)$$

Here, R and \dot{R} denote the oriented radii of the oriented spheres, where the orientation of an oriented sphere is encoded in the sign of its radius. In this sense, the transformation in Equation (10.1) is just a Laguerre (offset-) transformation from the point of view of Laguerre geometry, see [ADM⁺24]. From Equation (10.1) we obtain the following corollary.

Corollary 10.5. *Let c^φ be an associated congruence. Then there is a null congruence \dot{c}^φ with $\odot\dot{c}^\varphi = \odot c^\varphi$, see Figure 7 (right). \blacksquare*

In particular, this means that for every member h^φ of the associated family of a maximal surface there are two corresponding null congruences $(\dot{c}^1)^\varphi$, $(\dot{c}^2)^\varphi$.

Remark 10.6. Corollary 10.5 implies that every maximal incircular net p also comes with an associated family of two incircular nets $(p^1)^\varphi$, $(p^2)^\varphi$ that are the projections of $(\dot{c}^1)^\varphi$ and $(\dot{c}^2)^\varphi$, see Figure 8 (right). These are not isothermic incircular nets. Instead, $(p^1)^\varphi$ has the property that around each black vertex b the other tangents (as in Definition 4.4) are in oriented contact with an oriented circle of radius $2 \sin \varphi$ and center $(\odot p^2)^\varphi(b)$, and analogously for $(p^2)^\varphi$. It is not clear if this is a characterizing property for incircular nets in an associated family. This is in part because there currently is also no characterization of S-isothermic nets that are in an associated family. The projections of the contact congruences $(c^1)^\varphi$ and $(c^2)^\varphi$ were introduced in [ADM⁺24] as so called *cycle patterns* and are shown in Figure 8 (left). \blacksquare

Remark 10.7. In [ADM⁺24] we also discussed Miquel dynamics applied to contact congruences using some Lorentz Lie sphere geometry. With the arguments developed there it is possible to obtain a calculation-free proof of Theorem 10.4 as follows: the four oriented timelike Lorentz spheres that are cyclically in contact span a 3-space of signature $(++--)$ in the Lie lift. Therefore the polar complement of this span is a line of signature $(+-)$ which intersects the Lie quadric twice. These two intersection points correspond to two oriented timelike spheres that are in oriented contact with the original four oriented timelike spheres. However, we did not obtain a proof of the constant radii without the calculations above. Moreover, it is not hard to see that the two contact congruences c^1, c^2 in Theorem 10.4 are actually related by one step of Miquel

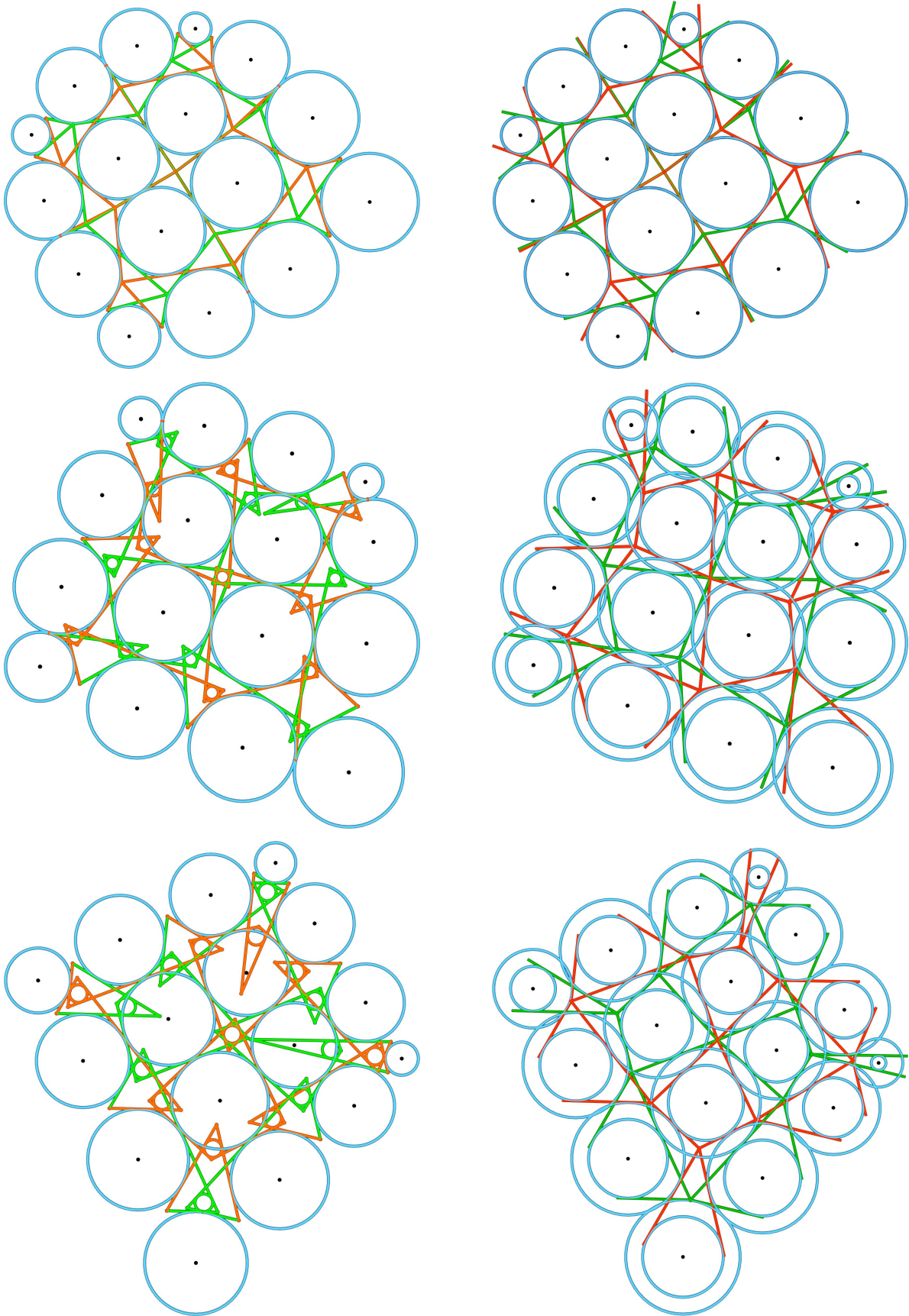


Figure 8: Planar nets obtained from the associated congruences in the associated family of a maximal surface (see Figure 7) for the values $\varphi = 0, \frac{\pi}{4}, \frac{\pi}{2}$, from top to bottom. Left: Projections of the isotropic lines and timelike spheres in the associated contact congruences $(c^1)^\varphi$ (green) and $(c^2)^\varphi$ (orange). All the green and orange circles have radius $\sin \varphi$. Right: The incircular nets obtained as projections of the associated null congruences $(\dot{c}^1)^\varphi$ (green) and $(\dot{c}^2)^\varphi$ (red).

dynamics. Furthermore, due to Corollary 10.5 it follows that iterated Miquel dynamics applied to associated congruences produces the sequence

$$\dots \leftrightarrow \odot c^\varphi \leftrightarrow \odot c^\varphi \leftrightarrow \mathcal{M}(\odot c^\varphi) \leftrightarrow \mathcal{M}(\odot c^\varphi) \leftrightarrow \odot c^\varphi \leftrightarrow \odot c^\varphi \leftrightarrow \mathcal{M}(\odot c^\varphi) \leftrightarrow \mathcal{M}(\odot c^\varphi) \leftrightarrow \dots$$

This is the same behaviour as we showed in [ADM⁺24] for isothermic congruences, except that for isothermic congruences it holds not just for the centers but also for the radii. It is currently unclear whether this type of Miquel sequence is characteristic for associated congruences. ■

11 The X -variables in the associated family

We begin by considering a vertex star of h_\circ in contrast to the quad of h_\circ we considered in Section 9. Let P_0, P_1, \dots, P_4 be five points such that the four edges P_0P_i for $i = 1, 2, 3, 4$ are tangent to \mathbf{U}_+ . Let T_1, T_2, T_3, T_4 be the corresponding unit edge vectors, R_i the radii of the spheres at the vertices, so that

$$P_i - P_0 = (R_i + R_0)T_i.$$

Let K_i be the touching point on the edge P_0P_i , so that $K_i - P_0 = R_0T_i$.

As before, the dual points are defined by

$$P_i^* - P_0^* = \pm(R_i^{-1} + R_0^{-1})T_i = (R_i^* + R_0^*)T_i^*,$$

where the sign is $+$ for horizontal edges and $-$ for vertical edges. The dual contact points satisfy $K_i^* - P_0^* = R_0^*T_i^*$.

The dual points in the vertex star of the associated family are obtained by integrating

$$P_i^\varphi - P_0^\varphi = \pm(R_i^* + R_0^*)T_i^\varphi$$

with T_i^φ determined by (9.1).

Note that the face normal n in (9.1) is not the same for the unit edge vectors $T_1^\varphi, T_2^\varphi, T_3^\varphi, T_4^\varphi$ of the vertex star. One can derive formulas for T_i^φ, N_i^φ and B_i^φ , analogous to (9.1), (9.2) and (9.3), for a vertex star of h_\circ . Instead of the face normal(s) n , one considers the vertex normal n_0 at P_0 , given by the connection of the center of \mathbf{U}_+ and P_0 . Then one can express T_i^φ, N_i^φ and B_i^φ in the orthonormal basis (t_i, n_0, B_i) where t_i is given by $t_i := n_0 \times B_i$ so that

$$\begin{aligned} T_i^\varphi &= t_i \cosh \theta \cos \varphi + n_0 \sinh \theta \cos \varphi + B_i \sin \varphi, \\ N_i^\varphi &= t_i \sinh \theta + n_0 \cosh \theta, \\ B_i^\varphi &= -t_i \cosh \theta \sin \varphi - n_0 \sinh \theta \sin \varphi + B_i \cos \varphi. \end{aligned}$$

Here θ is the angle that rotates (T_i, N_i, B_i) onto (t_i, n_0, B_i) and is given by $\tanh \theta = R_0$, in particular it independent of i .

The contact points K_i^φ of the surface in the associated family are given by

$$K_i^\varphi = \pm T_i^\varphi R_0^*,$$

where the sign depends on the type of edge. The direction vectors of the two isotropic lines $G_{i,\pm}^\varphi$ at K_i^φ are again given by $N_i^\varphi \pm B_i^\varphi$. The isotropic line $G_{i,+}^\varphi$ through K_i^φ intersects the isotropic line $G_{i+1,+}^\varphi$ through K_{i+1}^φ in a point Y_i . Indeed, they lie in two touching timelike spheres, the sphere of radius R_0^* centered at P_0^* , and the sphere of radius $\sin \varphi$ associated to the common adjacent face (see Figure 7, left), and therefore must intersect.

Let Π_0 be the tangent plane at P_0^* , that is the plane orthogonal to n_0 passing through P_0^* .

Lemma 11.1. *Let Z_i be the projection of the intersection point Y_i of consecutive isotropic lines onto the plane Π_0 . The distance of Z_i to P_0^* is independent of φ . In particular, it is given by*

$$|Z_i - P_0^*| = \frac{R_0^*}{\cos(\alpha/2)},$$

where α is the angle between t_i and t_{i+1} . ■

Proof. The intersection of Π_0 with the sphere around P_0^* is a circle of Radius R_0^* . An isotropic line contained in the sphere intersects this circle in a point V . Since the isotropic line lies in the tangent plane at V it projects to the tangent of the circle at V . Obviously, the distance of V to P_0^* is R_0^* . Hence, the projections of the isotropic lines are tangent to a circle with center P_0^* and radius R_0^* . The distance of their intersection point Z_i only depends on the angle the projected tangents form which is given by α . To show that the angle α is indeed also independent of φ , we consider the projections of the isotropic lines $G_{i,\pm}^\varphi$ to Π_0 , which in the orthonormal basis (t_i, n_0, B_i) have the direction vectors

$$t_i(\sinh \theta \mp \cosh \theta \sin \varphi) \pm B_i \cos \varphi.$$

Thus the angle α is simply the angle $\alpha = \angle(t_i, t_{i+1}) = \angle(B_i, B_{i+1})$. Consequently, the distance is given by $R_0^*/\cos(\alpha/2)$. □

We are ready to prove the final theorem.

Theorem 11.2. *The X -variables in the associated family of null congruences \check{c}^φ of a maximal congruence c do not depend on φ .* ■

Proof. We consider a family of null congruences \check{c}^φ and their projection to \mathbf{E}^2 , see also Figure 8 (right). Recall that due to Definition 4.2 we have that

$$X_\circ(w) = -\frac{(p_\bullet(b_1) - \odot p_\circ(w))(p_\bullet(b_2) - \odot p_\circ(w))}{(p_\bullet(b_3) - \odot p_\circ(w))(p_\bullet(b_4) - \odot p_\circ(w))}, \quad (11.1)$$

where $\odot p_\circ(w)$ is the projection of $\check{c}_\circ^\varphi(w)$ to \mathbf{E}^2 and $p_\bullet(b_i)$ is the projection of $\check{c}_\bullet^\varphi(b_i)$ to \mathbf{E}^2 . Moreover, there is a scaling of \mathbf{L}^3 centered at $\check{c}_\circ^\varphi(w)$ that takes the four points $\check{c}_\bullet^\varphi(b_i)$ to the respective contact points K_i of $c_\circ(w)$ with $c_\bullet(b_i)$. Hence, we may calculate $X_\circ(w)$ using the projections L_i^φ of the contact points K_i^φ via

$$X_\circ(w) = -\frac{(L_1^\varphi - \odot p_\circ(w))(L_2^\varphi - \odot p_\circ(w))}{(L_3^\varphi - \odot p_\circ(w))(L_4^\varphi - \odot p_\circ(w))},$$

because Equation (11.1) is manifestly invariant under scaling. Furthermore, due to Lemma 4.3 the X -variables are Lorentz invariant, thus we can also project to any other spacelike plane instead (of $\mathbf{E}^2 \subset \mathbf{L}^3$). With this in mind, we project the four contact points K_i^φ to the plane Π_0 of Lemma 11.1 instead of \mathbf{E}^2 . This yields exactly the points Z_i of Lemma 11.1. Thus, with $\odot \check{p}_\circ^\varphi(w) = \odot p_\circ^\varphi(w) = P_0^*$ we obtain the expression

$$X_\circ(w) = -\frac{(Z_1 - P_0^*)(Z_2 - P_0^*)}{(Z_3 - P_0^*)(Z_4 - P_0^*)}.$$

Finally, Lemma 11.1 shows that the distances of Z_i to $\odot p_\circ(w) = P_0^*$ are independent of φ , hence so are the X -variables. □

Remark 11.3. In [ADM⁺24] we defined the X -variables for a general contact congruence, and we showed that the X -variables are independent of Laguerre transformations. Since c^φ is related to \check{c}^φ by a Laguerre transformation, the X -variables of c^φ coincide with those of \check{c}^φ and therefore also do not depend on φ . ■

Remark 11.4. Theorem 11.2 implies that the X -variables for the incircular nets in the associated family of a maximal incircular net are independent of φ . Thus each maximal incircular net comes with a pair of 1-parameter families of incircular nets that have the same X -variables, and have the properties as discussed in Remark 10.6. ■

Remark 11.5. For isothermic incircular nets, we showed in [ADM⁺24] that the X -variables are in a subvariety, which we called the *isothermic subvariety*. Theorem 11.2 shows that the associated incircular nets also have X -variables in the isothermic subvariety, but they are not isothermic incircular nets. That said, the name *isothermic subvariety* may still be justified, since each c^φ is *still* an isothermic surface. The associated congruences are still discretizations of isothermic surfaces, just not in curvature-line parametrization. Moreover, as shown in [ADM⁺24] the isothermic subvariety is a characterization of a certain periodicity in the Miquel dynamics, see also Remark 10.7. In fact, it follows from the properties of the incircular nets p^φ in the associated family, that their center nets $\odot p^\varphi$ have the same periodicity behaviour with respect to Miquel dynamics. However, it is currently unclear how the radii behave under Miquel dynamics. ■

References

- [ADM⁺24] Niklas C. Affolter, Felix Dellinger, Christian Müller, Denis Polly, and Nina Smeenk. Discrete Lorentz surfaces and s-embeddings I: isothermic surfaces, 2024. Preprint, arXiv:2410.11575.
- [BH16] Alexander I. Bobenko and Tim Hoffmann. S-conical cmc surfaces. towards a unified theory of discrete surfaces with constant mean curvature. In Alexander I. Bobenko, editor, *Advances in Discrete Differential Geometry*, pages 287–308. Springer Berlin Heidelberg, Berlin, Heidelberg, 2016.
- [BHS06] Alexander I. Bobenko, Tim Hoffmann, and Boris A. Springborn. Minimal surfaces from circle patterns: Geometry from combinatorics. *Ann. Math. (2)*, 164(1):231–264, 2006.
- [BHS24] Alexander I. Bobenko, Tim Hoffmann, and Nina Smeenk. Constant mean curvature surfaces from ring patterns: Geometry from combinatorics, 2024. Preprint, arXiv:2410.08915.
- [BP99] Alexander I. Bobenko and Ulrich Pinkall. Discretization of surfaces and integrable systems. In Alexander I. Bobenko and Ruedi Seiler, editors, *Discrete integrable Geometry and Physics*, pages 3–58. Clarendon Press, Oxford, 1999.
- [BPW10] Alexander I. Bobenko, Helmut Pottmann, and Johannes Wallner. A curvature theory for discrete surfaces based on mesh parallelity. *Mathematische Annalen*, 348(1):1–24, Sep 2010.
- [BS04] Alexander I. Bobenko and Boris A. Springborn. Variational principles for circle patterns and Koebe’s theorem. *Trans. Amer. Math. Soc.*, 356(2):659–689, 2004.
- [BS08] Alexander I. Bobenko and Yuri B. Suris. *Discrete differential geometry: Integrable structure*, volume 98 of *Graduate studies in mathematics*. American Math. Soc., 2008.
- [Che18] Dmitry Chelkak. Planar Ising model at criticality: state-of-the-art and perspectives. In *Proceedings of the International Congress of Mathematicians—Rio de Janeiro 2018. Vol. IV. Invited lectures*, pages 2801–2828. World Sci. Publ., Hackensack, NJ, 2018.

- [CLR21] Dmitry Chelkak, Benoît Laslier, and Marianna Russkikh. Bipartite dimer model: perfect t-embeddings and Lorentz-minimal surfaces, 2021. Preprint, arXiv:2109.06272.
- [CLR23] Dmitry Chelkak, Benoît Laslier, and Marianna Russkikh. Dimer model and holomorphic functions on t-embeddings of planar graphs. *Proceedings of the London Mathematical Society*, 126(5):1656–1739, 2023.
- [DS97] Adam Doliwa and Paolo M. Santini. Multidimensional quadrilateral lattices are integrable. *Physics Letters A*, 233(4):365 – 372, 1997.
- [KLRR22] Richard Kenyon, Wai Yeung Lam, Sanjay Ramassamy, and Marianna Russkikh. Dimers and circle patterns. *Annales Scientifiques de l'École Normale Supérieure*, 55(3):863–901, 2022.
- [Kob83] Osamu Kobayashi. Maximal surfaces in the 3-dimensional Minkowski space L^3 . *Tokyo Journal of Mathematics*, 06(2):297–309, 1983.
- [LPW⁺06] Yang Liu, Helmut Pottmann, Johannes Wallner, Yongliang Yang, and Wenping Wang. Geometric modeling with conical meshes and developable surfaces. *ACM Transactions on Graphics*, 25(3):681–689, 7 2006.
- [Pem20] Mason Pember. Weierstrass-type representations. *Geometriae Dedicata*, 204(1):299–309, 2020.
- [Sau33] Robert Sauer. Wackelige Kurvennetze bei einer infinitesimalen Flächenverbiegung. *Mathematische Annalen*, 108(1):673–693, 1933.
- [Sch97] Oded Schramm. Circle patterns with the combinatorics of the square grid. *Duke Math. J.*, 86(2):347–389, 1997.
- [Sch03] Wolfgang K. Schief. On the unification of classical and novel integrable surfaces. II. Difference geometry. *R. Soc. Lond. Proc. Ser. A Math. Phys. Eng. Sci.*, 459(2030):373–391, 2003.
- [Sch06] Wolfgang K. Schief. On a maximum principle for minimal surfaces and their integrable discrete counterparts. *Journal of Geometry and Physics*, 56(9):1484–1495, 2006.